Colloids and Surfaces B: Biointerfaces 87 (2011) 151–158

Contents lists available at ScienceDirect

Colloids and Surfaces B: Biointerfaces

journal homepage: www.elsevier.com/locate/colsurfb

Influence of natural organic matter on the deposition kinetics of extracellular polymeric substances (EPS) on silica

Meiping Tong[a,*], Pingting Zhu[a], Xujia Jiang[a], Hyunjung Kim[b,**]

[a] The Key Laboratory of Water and Sediment Sciences, Ministry of Education, College of Environmental Sciences and Engineering, Peking University, Beijing 100871, PR China
[b] Department of Mineral Resources and Energy Engineering, Chonbuk National University, 664-14 Duckjin-Dong 1Ga, Jeonju, Jeonbuk 561-756, Republic of Korea

ARTICLE INFO

Article history:
Received 24 January 2011
Received in revised form 8 April 2011
Accepted 7 May 2011
Available online 18 May 2011

Keywords:
Extracellular polymeric substances (EPS)
Deposition kinetics
Natural organic matter (NOM)
Electrophoretic mobility
Quartz crystal microbalance with dissipation (QCM-D)

ABSTRACT

The influence of humic acid and alginate, two major components of natural organic matter (NOM), on deposition kinetics of extracellular polymeric substances (EPS) on silica was examined in both NaCl and $CaCl_2$ solutions over a wide range of environmentally relevant ionic strengths utilizing a quartz crystal microbalance with dissipation. Deposition kinetics of both soluble EPS and bound EPS extracted from four bacterial strains with different characteristics was investigated. EPS deposition on humic acid-coated silica surfaces was found to be much lower than that on bare silica surfaces under all examined conditions. In contrast, pre-coating the silica surfaces with alginate enhanced EPS deposition in both NaCl and $CaCl_2$ solutions. More repulsive electrostatic interaction between EPS and surface contributed to the reduced EPS deposition on humic acid-coated silica surface. The trapping effect induced by the rough alginate layer resulted in the greater EPS deposition on alginate-coated surfaces in NaCl solutions, whereas surface heterogeneities on alginate layer facilitated favorable interactions with EPS in $CaCl_2$ solutions. The presence of dissolved background humic acid and alginate in solutions both significantly retarded EPS deposition on silica surfaces due to the greater steric and electrostatics repulsion.

1. Introduction

Bacteria are ubiquitous microorganisms present in natural environment. They have great significances in geochemical processes such as soil formation [1] and nutrients cycling [2]. Due to their unique capabilities of contaminant accumulation and degradation, bacteria are also widely applied for industrial uses in water and wastewater treatment processes [3,4]. Extracellular polymeric substances (EPS), biomacromolecules located on or around cell surface and secreted during bacteria growth, have been found to play crucial roles in mineral dissolution and the formation of soil through different interactions with clay mineral particles [5,6]. Many studies also reported that EPS had important impact on the processes of pollutant accumulation and degradation via cross-linked formation of polymeric networks that were capable of adsorbing organic pollutants and heavy metals [7–9].

EPS are a complex mixture of high molecular weight organic compounds such as polysaccharides, proteins, humic acids as well as other non-polymeric components of low molecular weight [10–12]. These compositions contain a variety of functional groups such as carboxyl, hydroxyl, phosphate, amino groups, and so on [13]. As a result, EPS can interact with various substances present in surrounding environment and play important roles in the above mentioned processes (e.g. mineral dissolution and pollutants degradation). Interaction of EPS with surfaces (deposition of EPS to surfaces) has recently also been shown to significantly influence the formation of biofilms [14,15] and cell transport behavior [16–20], thus eventually affect the successful application of bioremediation. Understanding the deposition kinetics of EPS on surfaces is therefore necessary to control the transport of microbes and the formation of biofilms.

However, only a few studies have investigated the deposition kinetics of EPS on mineral surfaces. By employment of attenuated total internal reflection infrared spectroscopy (ATR-FTIR), Omoike et al. [21] examined the interaction of EPS with goethite (α-FeOOH) surface. Kwon et al. [22] utilized quartz crystal microbalance with dissipation (QCM-D) to investigate the deposition of dextran (chosen to represent polysaccharides in EPS) on alumina and silica. Subsequently, using atomic force microscopy (AFM), Kwon et al. [13] compared the interactions of silica surfaces with three different homopolymers selected to represent different components of EPS. Very recently, Zhu et al. [23] employed QCM-D to investigate the deposition kinetics of EPS on silica surface under a wide range of environmentally relevant solution ionic strengths and pH.

* Corresponding author. Tel.: +86 10 62756491; fax: +86 10 62756526.
** Corresponding author. Tel.: +82 63 2702370; fax: +82 63 2702366.
E-mail addresses: tongmeiping@iee.pku.edu.cn (M. Tong), kshjkim@jbnu.ac.kr (H. Kim).

0927-7765/$ – see front matter © 2011 Elsevier B.V. All rights reserved.
doi:10.1016/j.colsurfb.2011.05.015

These above studies investigated the deposition of EPS in simplified systems using mineral surface as a surrogate for the solid–liquid interface. However, in natural environment, mineral surfaces (e.g. silica surfaces) are commonly covered by natural organic matter (NOM). Previous studies have shown that NOM pre-coating on surfaces would significantly affect the deposition behaviors of biological colloids and nanoparticles [24–26]. Moreover, NOM is also ubiquitous present in the aqueous phase, ranging from a few mg L^{-1} to a few hundred mg L^{-1} C [27]. The dissolved NOM is known to readily adsorb to colloidal particles and enhance colloid stability in water, thus affect their deposition on surfaces [26]. To date, the influence of natural organic matter (in solid or aqueous phase) on the deposition kinetics of EPS yet has not been well explored, and requires investigation.

The objective of this paper is to systematically examine the influence of NOM (both dissolved in solutions and adsorbed on silica surfaces) on the deposition kinetics of EPS. Eight EPS: both soluble EPS (SEPS) and bound EPS (BEPS) (SEPS and BEPS can be classified according to their relative proximity to the bacterial cell surface) extracted from four bacterial strains with different characteristics were investigated in this study. The significance of humic acid and alginate (two major components of NOM) on the deposition kinetics of EPS was determined over a wide range of environmentally relevant ionic strengths (1, 10, 50 mM NaCl and 0.3, 0.6, 1 mM $CaCl_2$) employing a quartz crystal microbalance with dissipation (QCM-D). Our study showed that deposition of EPS on silica surfaces could be significantly influenced by NOM (humic acid and alginate) either dissolved in solutions or adsorbed on silica surfaces under solution conditions relevant to subsurface environment.

2. Materials and methods

2.1. EPS preparation

SEPS and BEPS were extracted from four bacterial strains: *Escherichia coli* BL21 (gram-negative, non-motile), *Pseudomonas* sp. QG6 (gram-negative, motile), *Rhodococcus* sp. QL2 (gram-positive, non-motile), and *Bacillus subtilis* (gram-positive, motile). Bacteria were grown and harvested according to protocols described in previous publications [20,23] as well as in the Supplementary Information. After harvest, the cell pellets were re-suspended in Milli-Q water for the subsequent EPS extraction process. SEPS were separated via a centrifugation at 4000 rpm for 20 min at 4 °C. Following the SEPS extraction, the pellets were re-suspended in Milli-Q water and the cell suspension was then transferred to a sterilized extraction beaker to release BEPS via cation exchange resin technique developed by Frolund et al. [11]. CER (Dowex Marathon C, 20–50 mesh, sodium form, Fluka 91973), which was soaked in Milli-Q water overnight prior to use, was added to the extraction beaker with a dosage of 2.5 g g^{-1} bacterial mass. The bacteria–CER suspension was then stirred at 600 rpm for 1.5 h at 4 °C. This was followed by a settlement of the suspension for 3 min to separate CER. The extracted BEPS were collected by centrifugation at 8000 rpm for 20 min at 4 °C. Both extracted SEPS and BEPS were filtrated through sterilized 0.22 μm cellulose acetate filters to remove residuals and bacterial cells. The obtained EPS were then divided into several portions and stored in sterilized bottles at −18 °C. Aliquots of EPS solutions were taken out of the freezer and allowed to warm up to room temperature immediately before electrophoretic mobility measurements and QCM-D experiments. Detailed electrophoretic mobility measurements of all types of EPS are provided in the Supplementary Information.

2.2. NOM solutions preparation

Suwannee River humic acid (SRHA) (Cat#2S101H, Standard II, International Humic Substances Society), the most abundant NOM in freshwater systems [28] and has been previously used as model NOM in many studies [29–31], was employed to model humic substances in this study. Alginates (A2158, Sigma–Aldrich, St. Louis, MO), polysaccharides commonly found in marine environments [32,33] and have also been widely employed to represent polysaccharides [34], were used to model polysaccharides in this study. The MWs of the SRHA and alginate used in this study are 1–5 and 12–80 kDa, respectively. The SRHA stock solution was prepared by dissolving 25.0 mg of dry SRHA powder in 50 mL Milli-Q water (Q-Gard1, Millipore Inc., MA) and stirring the solution for 24 h. The alginate stock solution was made by dissolving 1.60 g of dry sodium alginate powder in 480 mL of Milli-Q water and stirring the solution for 48 h. Both solutions were then filtered through 0.22 μm cellulose acetate membranes under vacuum. The pH of both solutions was adjusted to 6.0 by adding 0.1 M NaOH. The TOC content of the humic acid and alginate stock solutions was found to be 235.1 and 967.0 mg L^{-1} using a TOC-meter (Tekmer Fusion, Teledyne Instruments, CA), respectively. Both stock solutions were stored in the dark at 4 °C until use.

2.3. Quartz crystal microbalance with dissipation (QCM-D)

A QCM-D E1 system (Q-Sense AB, Gothenburg, Sweden) was utilized to examine the influence of NOM (both dissolved in solutions and adsorbed on silica surfaces) on the deposition kinetics of EPS on silica surfaces. QCM-D experiments were preformed with 5 MHz AT-cut quartz sensor crystals with silica-coated surface (Batch 081110). Before each measurement, the crystals were soaked 30 min in a 2% SDS solution, rinsed thoroughly with Milli-Q water, dried with ultrahigh-purity N_2 gas, and then oxidized for 30 min in a UV/O_3 chamber (Bioforce Nanosciences, Inc., Ames, IA) [35,36]. The radial stagnation point flow configuration of measurement chamber allows the fluid to be directly flowed toward the center of crystal surface, and then flowed out from the edges via using a peristaltic pump (ISMATEC, Switzerland) operating in clockwise mode. Specifically, the pump was connected to the sensor crystal outlet, and the studied solutions, stored in a sterilized 50 mL polypropylene conical tube (Becton Dickinson, NJ) connected to the sensor crystal inlet, were fed through the crystal sensor chamber at a flow rate of 0.1 mL min^{-1}. This flow rate could result in laminar flow in the chamber [26].

2.4. EPS deposition experiments

The influence of NOM, both adsorbed on silica surfaces and dissolved in solutions, on the deposition kinetics of EPS was examined in this study. To investigate the significance of adsorbed NOM on the deposition kinetics of EPS, deposition behavior of EPS on silica surfaces, poly-L-lysine (PLL) hydrobromide coated surfaces (PLL, molecular weight of 70,000–150,000, P-1274, Sigma–Aldrich, St. Louis, MO), and NOM-coated surfaces was examined over a wide range of environmentally relevant ionic strength in both NaCl (ranging from 1 to 200 mM) and $CaCl_2$ solutions (ranging from 0.3 to 5 mM) at pH 6.0 (adjusted with 0.1 M HCl or 0.1 M NaOH). This wide range of solution chemistries examined in this study can be commonly found in groundwater [e.g. Refs. 37,38].

For the experiments conducted on bare silica surfaces, the QCM-D system was pre-equilibrated with desired salt solution for a minimum of 30 min to establish a stable baseline. After pre-equilibration, an EPS suspension (70 ± 1.0 mg L^{-1}) at desired ionic strength was injected into the crystal chamber. The duration of injection lasted for at least 30 min.

For the experiments conducted on favorable (non-repulsive) condition, a layer of positively charged PLL was deposited on silica surfaces prior to the deposition experiments. We followed the method that employed in previous works to adsorb a layer of PLL onto the silica surface [39,40], which was also provided in the Supplementary Information. Corresponding deposition experiments on PLL-coated silica surfaces were performed over the same ionic strength range in both NaCl and $CaCl_2$ solutions with the same EPS influent concentration as that conducted on bare silica surfaces. A detail about EPS deposition experiment on PLL-coated surfaces was also provided in the Supplementary Information.

For deposition experiments conducted on NOM (SRHA or alginate) coated silica surfaces, the bare silica surfaces were first modified with a layer of positively charged PLL, and then a negative charged NOM (SRHA or alginate) solution at 30 mg L^{-1} TOC prepared in 1 mM NaCl solution was flowed across the crystal to form a NOM layer on PLL-coated silica. Details of adsorbing NOM layer on PLL-coated can be found in the Supplementary Information. After coating the surfaces with NOM, the salt solution of interest was flowed through the NOM-coated surface until a constant baseline was obtained, which was followed by the injection of the desired EPS sample containing 70 ± 1.0 mg L^{-1} TOC EPS with the same solution ionic strength into the flow chamber.

To examine the influence of dissolved NOM on the deposition kinetics of EPS, deposition experiments were conducted on bare silica surfaces in the presence of background SRHA or alginate (1 mg L^{-1} TOC) over a wide range of environmentally relevant ionic strength in both NaCl solutions and $CaCl_2$ solutions at pH 6.0. Prior to these deposition experiments, the bare silica surface was rinsed with salt solution of interest, followed by NOM solution (SRHA or alginate, 1 mg L^{-1} TOC) with the same ionic strength for at least 1 h to establish the stable baseline. EPS solution containing 70 ± 1.0 mg L^{-1} TOC EPS and 1 mg L^{-1} TOC of SRHA or alginate with the same solution ionic strength was then introduced into the measurement chamber for the deposition experiment.

2.5. QCM-D data analysis

For all the experiments, the deposition rate can be determined from the slope of the initial (linear) portion of the change in normalized frequency Δf_3 versus time curve [35,39]:

$$k_f = \frac{d\Delta f_3}{dt} \quad (1)$$

The deposition rate at different solution conditions is then presented in terms of the deposition efficiency (α), which is the ratio of the deposition rate in the presence of an energy barrier (k_{fp}) relative to the corresponding deposition rate in the absence of an energy barrier (k_{fa}) (favorable condition):

$$\alpha = \frac{k_{fp}}{k_{fa}} \quad (2)$$

2.6. DLVO interaction force

DLVO theory was used to calculate the total interaction force between EPS and substrate surface as a function of separation distance. van der Waals and electrical double layer forces were considered in DLVO theory. The particle-collector interaction force was calculated by treating the particle-collector system as a sphere–plate interaction. The retarded van der Waals forces for sphere–plate configuration can be calculated according to the following equation [41]:

$$F_{vdw} = -\frac{A_{132} a_p \lambda (\lambda + 22.232h)}{6h^2(\lambda + 11.116h)^2} \quad (3)$$

where a_p refers to the size of EPS, which was taken from values measured by Zetasizer Nano ZS90 (Malvern Instruments, UK); h is the separation distance between EPS and plate surface; λ is the characteristic wavelength of interaction, usually taken as 100 nm; A_{132} is the combined Hamaker constant for the particle–water–surface system, which can be calculated from the Hamaker constant of the individual material by following equation [42,43]:

$$A_{132} = (\sqrt{A_{11}} - \sqrt{A_{33}})(\sqrt{A_{22}} - \sqrt{A_{33}}) \quad (4)$$

where A_{11} is the Hamaker constant for EPS. Since the dominant component of all eight examined EPS was protein [23], the Hamaker constant for BSA (7.78×10^{-20} J) [44] was used to represent Hamaker constant for EPS in the absence of NOM in the solutions. Adsorption of NOM to EPS would occur when NOM is present in EPS solutions, thus the Hamaker constant for NOM (humic acid) (4.85×10^{-20} J) [45] is employed to represent the Hamaker constant for EPS when NOM is present in the solutions. A_{22} is the Hamaker constant for collector surface. For bare silica, the Hamaker constant is taken from Israelachvili [43] as 6.50×10^{-20} J. For NOM-coated surface, 4.85×10^{-20} J [45] was utilized. A_{33} is the Hamaker constants for water and is also taken from Israelachvili [43] as 3.70×10^{-20} J. The result from Eq. (4) for the combined Hamaker constants for EPS–water–bare silica and EPS–water–NOM-coated surface systems without background NOM in solutions is 5.42×10^{-21} J and 2.41×10^{-21} J, respectively. Whereas, the combined Hamaker constants for EPS-water-silica system with background NOM in solutions is 1.74×10^{-21} J.

The electrostatic double layer forces for sphere–plate configurations can be determined according to the following equations [41]:

$$F_{EDL} = 4\pi\varepsilon_r\varepsilon_0\kappa a_p\zeta_p\zeta_c \left[\frac{\exp(-\kappa h)}{1+\exp(-\kappa h)} - \frac{(\zeta_p - \zeta_c)^2}{2\zeta_p\zeta_c}\frac{\exp(-2\kappa h)}{1-\exp(-2\kappa h)}\right] \quad (5)$$

$$\kappa = \sqrt{\frac{e^2 \sum n_{j0} z_j^2}{\varepsilon_0 \varepsilon_r kT}} \quad (6)$$

where ε_0 is the permittivity of vacuum; ε_ρ is the dielectric constant or relative permittivity of water; ζ_π and ζ_χ are the zeta potential of the EPS and the plate surface, respectively; z_j is the ion valence, e is the electron charge; n_{j0} is the number concentration of ions in the bulk solution.

3. Results and discussion

3.1. Electrophoretic mobility of EPS

The influence of solution ionic composition, ionic strength, and NOM on the electrophoretic mobilities and zeta potentials of both SEPS and BEPS extracted from four bacterial strains was examined. Fig. 1 presents the representative zeta potentials of EPS extracted from bacterial strain *E. coli* as a function of solution ionic strength at pH 6.0 both in the absence and presence of background NOM. The observed zeta potentials of both SEPS (Fig. 1, top) and BEPS (Fig. 1, bottom) both in the absence and presence of background NOM were negative and became less negative with increasing solution ionic strength in both NaCl (Fig. 1, left) and $CaCl_2$ (Fig. 1, right) solutions due to compression of the electrostatic double layer. Under the same ionic strength (i.e. 1 mM), zeta potentials of EPS both in the absence and presence of NOM in $CaCl_2$ solutions (Fig. 1, right) were less negative relative to those in NaCl solutions (Fig. 1, left), which was due to calcium cations complexing with EPS resulting in the neutralization of surface charge [46]. Close investigation of Fig. 1 showed that under the same ionic strength, zeta potentials for EPS with background SRHA (Fig. 1, open diamond) and alginate (Fig. 1, open triangle) were slightly more negative than those without

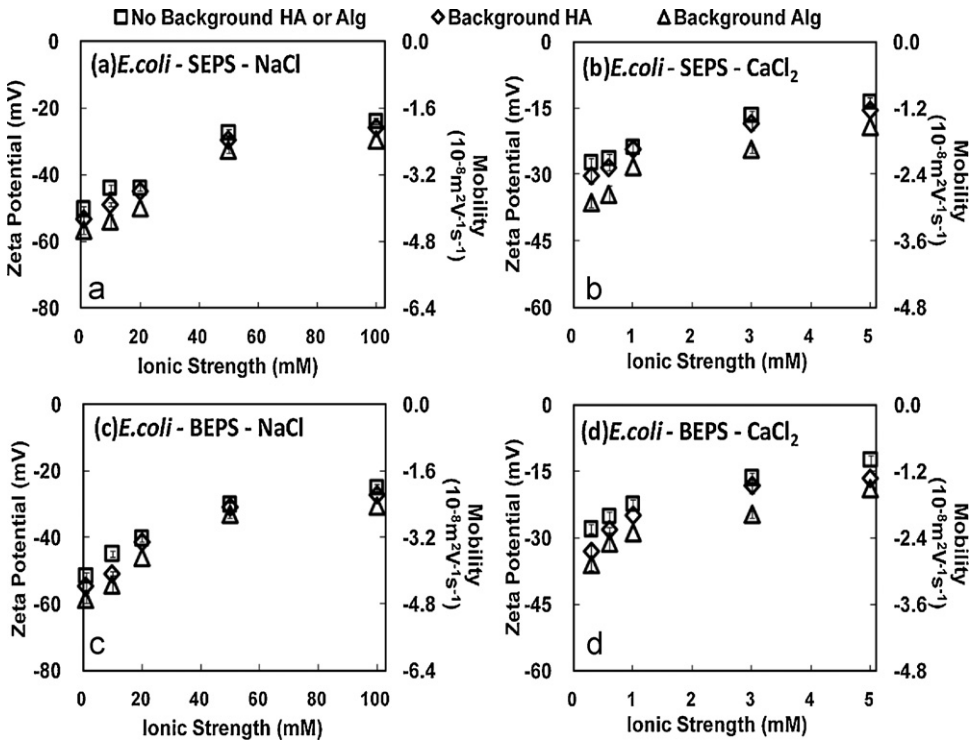

Fig. 1. Electrophoretic mobilities and zeta potentials of SEPS (a and b) and BEPS (c and d) for *E. coli* in the absence of NOM (open square) and in the presence of background humic acid (open diamond) and alginate (open triangle) in both NaCl (left) and $CaCl_2$ (right) solutions as a function of ionic strength at pH 6.0 (adjusted with 0.1 M HCl or 0.1 M NaOH). HA and Alg refer to humic acid and alginate, respectively. Error bars represent standard deviations of 6–12 measurements.

background NOM in both NaCl and $CaCl_2$ solutions. This was true for all examined ionic strengths. Adsorption of SRHA and alginate onto EPS surfaces would lower zeta potentials of EPS due to the more negative surface charge of these NOM molecules (Table S1). The zeta potentials of EPS with background alginate were slightly more negative than those with background SRHA, which were caused by the adsorption of more negatively charged alginate onto EPS surfaces (Table S1). These above observations were also true for EPS extracted from other three bacterial strains (Figs. S1 and S2). The results show that the presence of background NOM (SRHA or alginate) slightly decreases the zeta potentials of all eight examined EPS regardless they were extracted from different bacterial strains.

3.2. EPS deposition on bare silica surfaces

EPS deposition on bare silica surfaces was performed over a wide range of solution ionic strengths in both NaCl (with seven ionic strengths ranging from 1 to 200 mM) and $CaCl_2$ solutions (with five ionic strengths ranging from 0.3 to 5 mM) at pH 6.0. Deposition rates of EPS on bare silica surfaces obtained under these solution chemistry conditions were provided in Tables S2 and S3. EPS deposition kinetics on bare silica was also presented in terms of deposition efficiency (α), which can be derived by normalizing EPS deposition rates on bare silica surfaces by favorable deposition rates on PLL-coated surfaces at corresponding ionic strengths (Tables S2 and S3). Representative α of both SEPS and BEPS extracted from strain *E. coli* in both NaCl and $CaCl_2$ solutions at three selected solution ionic strengths were also provided in Fig. 2 (black bar). It can be clearly found from Table S2 and Fig. 2 (left, black bar) that in NaCl solutions, α of both SEPS and BEPS increased with increasing solution ionic strength. The same trend was also observed in $CaCl_2$ solutions (Table S3 and Fig. 2, right). This deposition behavior was consistent with the trends of zeta potentials of EPS versus ionic strength (Fig. 1) and thus generally agreed with classic Derjaguin–Landau–Verwey–Overbeek (DLVO) theory. The increase of solution ionic strength compressed electrostatic double layer between EPS and silica surface and thus resulted in greater deposition of EPS. Close comparison of α in $CaCl_2$ solutions with those in NaCl solutions yielded that α in $CaCl_2$ solutions were larger than those in NaCl solutions under the same examined ionic strength (i.e. 1 mM) (Tables S2 and S3 and Fig. 2). The result agreed with the less negative zeta potentials of EPS in $CaCl_2$ solutions relative to those in NaCl solutions (Fig. 1), thus also agreed with less repulsive electrostatic interaction between EPS and silica surface in $CaCl_2$ solutions (Fig. 3).

3.3. EPS deposition on NOM-coated silica surfaces

The deposition efficiencies (α) of representative SEPS and BEPS extracted from bacterial strain *E. coli* on SRHA-coated silica and alginate-coated silica surfaces at selected solution ionic strengths (1, 10, and 50 mM NaCl, 0.3, 0.6, and 1 mM $CaCl_2$) were presented in Figs. 2 and 4 (gray bar), respectively. At all solution ionic strengths examined, α for both SEPS and BEPS on the SRHA-coated silica surfaces (Fig. 2, gray bar) were about 1 order of magnitude lower than those on bare silica surfaces (Fig. 2, black bar) in both NaCl (Fig. 2, left) and $CaCl_2$ (Fig. 2, right) solutions. Under the same solution conditions, zeta potentials of SRHA were more negative than those of bare silica (Table S1). Therefore, it is expected that, in both NaCl and $CaCl_2$ solutions, the electrostatic double layer interaction force between EPS and SRHA-coated silica surface (Fig. 3a and b, upper, dot line) would be more repulsive relative to that between EPS and bare silica surface (Fig. 3a and b upper, dashed line). The expected more repulsive electrostatic interaction between EPS and SRHA-coated surface likely contributed to the obvious lower of α on SRHA-coated silica surface relative to that on bare silica. Under the same solution ionic strength (1 mM), α of EPS on SRHA-coated surfaces obtained in $CaCl_2$ solutions (Fig. 2, right, gray bar) was larger than that acquired in NaCl solutions (Fig. 2, left, gray bar), which can be explained by the less negative zeta potential (i.e.

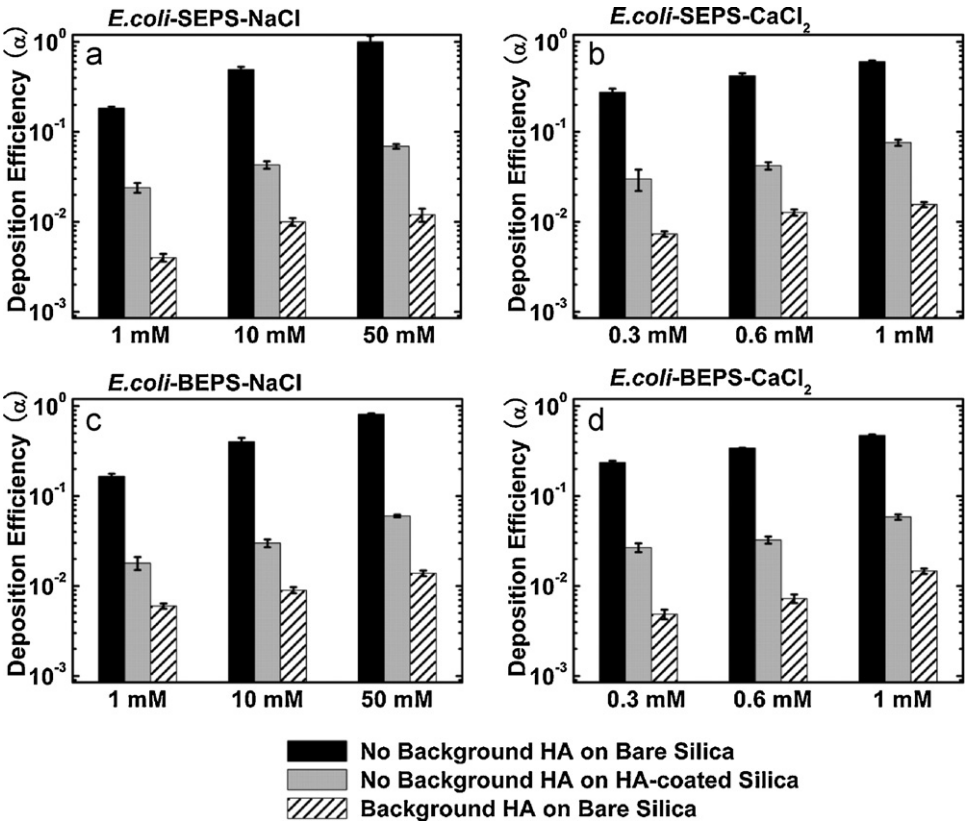

Fig. 2. Deposition efficiencies (α) of SEPS (a and b) and BEPS (c and d) extracted from *E. coli* in the absence of NOM on bare silica surfaces (black bar) and humic acid-coated silica surfaces (gray bar), and in the presence of background humic acid on bare silica surfaces (grid bar) as a function of ionic strength in NaCl (left) and $CaCl_2$ (right) solutions at pH 6.0 (adjusted with 0.1 M HCl or 0.1 M NaOH). HA refers to humic acid. Duplicate measurements were conducted over entire ionic strength range ($n \geq 2$), with error bars representing standard deviations.

less repulsive electrostatic double layer interaction force) between SRHA-coated surface and EPS in 1 mM $CaCl_2$ solutions than in 1 mM NaCl solutions (Fig. 3). Steric repulsion between EPS and SRHA-coated surface may also contribute to the drastic decrease of EPS deposition kinetics [47]. The retarded deposition kinetics on SRHA-coated silica surface also held true for both SEPS and BEPS extracted from other three bacterial strains (Figs. S3 and S4).

Similar to the observation for SRHA, zeta potentials of alginate were also more negative relative to those of bare silica under the same solution ionic strength in both NaCl and $CaCl_2$ solutions (Table S1). Thus, the electrostatic double-layer repulsion is expected to be greater between EPS and alginate-coated surface (Fig. 3c and d, dot line) than that between EPS and bare silica surface (Fig. 3c and d, dashed line), which would result in lower deposition kinetics of EPS on alginate-coated surfaces relative to that on bare silica. However, deviated from classic DLVO expectation (i.e. more negative surface leads to more repulsive electrostatic force between interacting particles), α for both SEPS and BEPS on the alginate-coated silica surfaces (Fig. 4, gray bar) were slightly larger than those on bare silica surfaces (Fig. 4, black bar) at all solution ionic strengths in NaCl solutions and at low ionic strengths in $CaCl_2$ solutions (0.3 and 0.6 mM $CaCl_2$). Obviously, unlike SRHA-coated surfaces, the deposition kinetics on alginate-coated surfaces was not mainly captured by classic DLVO theory (electrostatic interactions and van der Waals attraction) under these conditions. Other mechanisms should also play important roles in EPS deposition on alginate-coated surfaces. Since the alginate macromolecules were larger than humic acid, the adsorbed alginate could be in a more extended conformation from the surface of silica [26]. Thus at all examined ionic strengths in NaCl solutions (1, 10, and 50 mM), the coated alginate layer was likely to be much rougher compared to humic acid layer. This rough alginate-coated surface would allow EPS to be trapped within the alginate molecules (illustrated in the schematic of Fig. S5), resulting in the slightly larger α in NaCl solutions. The alginate layer surface is more compacted in $CaCl_2$ solutions [48,49], thus, the mechanism of EPS trapping undergoing in NaCl solutions would not occur in $CaCl_2$ solutions. The relatively higher α on alginate-coated surfaces at low ionic strengths in $CaCl_2$ solutions are likely due to the presence of heterogeneities on alginate-coated surface under these conditions [50,51], which could facilitate EPS deposition through favorable interactions with EPS, i.e. via hydrophobic interactions, hydrogen bonding, and local favorable electrostatic interactions. At high ionic strength in $CaCl_2$ solutions (1 mM), α on alginate-coated surfaces was equivalent as that on bare surfaces. Alginate would form complexes with calcium at high ionic strength in $CaCl_2$ solutions, resulting in the modification of the physical properties and surface morphology of the alginate layer [26,51,52]. This surface modification hindered EPS to reach local favorable deposition sites on alginate layer, thus the enhancement of EPS deposition was not so significant at 1 mM relative to that at low ionic strengths (0.3 and 0.6 mM). The enhanced deposition kinetics of EPS on alginate-coated surfaces also held true for both SEPS and BEPS extracted from other three bacterial strains (Figs. S6 and S7).

The above observations clearly showed that, for all eight examined EPS, pre-coating silica surfaces with SRHA would significantly retard deposition kinetics of EPS in both NaCl and $CaCl_2$ solutions, whereas, pre-coating silica surfaces with alginate would enhance

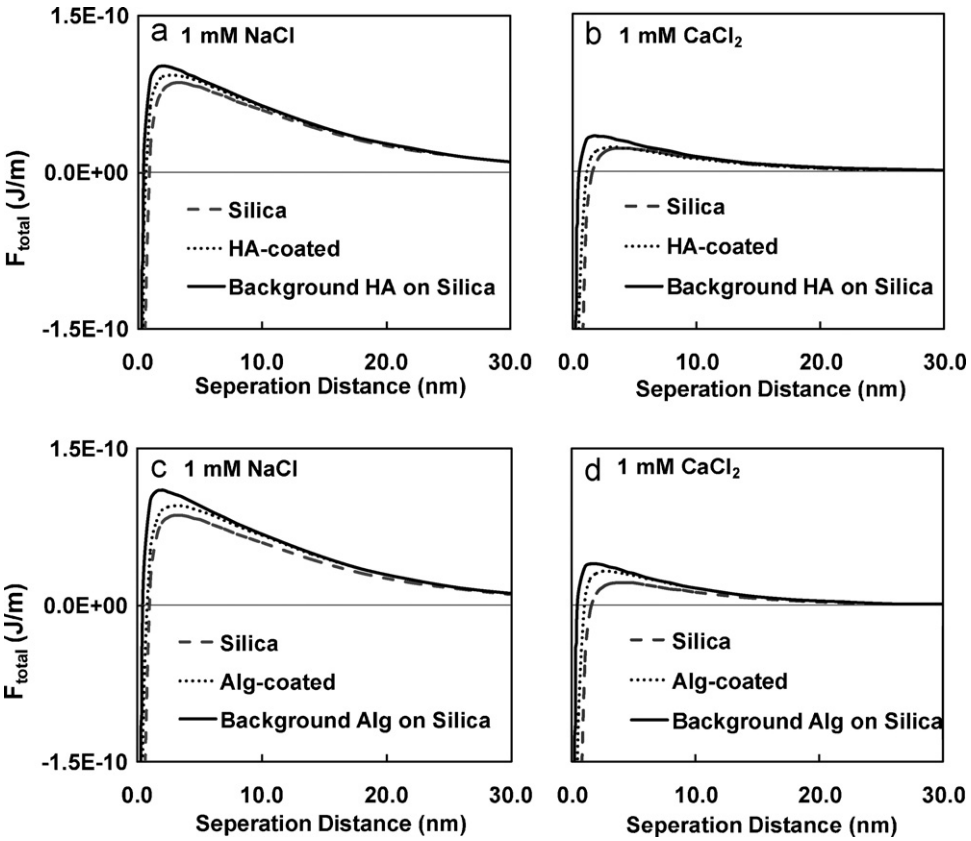

Fig. 3. DLVO interaction forces between EPS and bare silica surface in the presence and absence of background NOM and between EPS and NOM-coated surface in the absence of background NOM in 1 mM NaCl and 1 mM $CaCl_2$ solutions. The EPS size, zeta potentials of EPS and collectors utilized to calculate DLVO interaction forces are listed in Table S4.

the deposition of EPS. The results indicate that the adsorption of NOM on silica surfaces can either reduce or enhance the EPS deposition kinetics, depending on the surface morphology of the NOM macromolecules.

3.4. Influence of dissolved NOM on EPS deposition

EPS deposition experiments on bare silica were also performed in the presence of background NOM (SRHA or alginate) with the TOC concentration of 1 mg L^{-1} at selected solution ionic strengths in both NaCl and $CaCl_2$ solutions (1, 10, and 50 mM NaCl, 0.3, 0.6, and 1 mM $CaCl_2$). As described in Section 2, prior to these experiments, the bare silica surfaces were first rinsed with salt solutions of interest, and then followed by SRHA or alginate solution (1 mg L^{-1} TOC) with the same ionic strength. No significant frequency shifts were observed when NOM with NaCl solutions were introduced, indicating the absence of NOM adsorption on the silica surfaces in NaCl solutions. However, in the presence of $CaCl_2$, the frequency Δf_3 shifted about 8–10 Hz, suggesting significant adsorption of NOM on silica surfaces. The adsorption of NOM on silica surfaces during precondition process in $CaCl_2$ solutions has also been reported in previous study [26]. Adsorption of background NOM onto EPS surfaces occurred both in NaCl and $CaCl_2$ solutions, based on the observation of lower zeta potentials of EPS with the presence of NOM in solutions (Fig. 1).

α of both SEPS and BEPS from *E. coli* in the presence of background SRHA (Fig. 2, grid bar) was about 1–2 orders of magnitude lower than those in the absence of SRHA (Fig. 2, black bar) in both NaCl and $CaCl_2$ solutions. The adsorption of SRHA on EPS surfaces resulted in the more negative zeta potentials of EPS (SRHA-adsorbed EPS) relative to those without background SRHA in solution (bare EPS) (Fig. 1). Thus, the electrostatic interaction between EPS and silica (Fig. 3a and b, solid line) is expected to be more repulsive with the presence of background SRHA in solution than that with the absence of background SRHA (Fig. 3a and b, dashed line). This suggests that the more repulsive electrostatic interaction between SRHA-adsorbed EPS and silica surface would contribute to the observed significant decrease of deposition kinetics in the presence of background SRHA in NaCl solutions (Fig. 2, left). The steric repulsion between SRHA-adsorbed EPS and bare silica may also retard EPS deposition on bare silica surfaces in NaCl solutions. In $CaCl_2$ solutions, the observed decrease of EPS deposition kinetics with background SRHA was also caused by more repulsive electrostatic interaction with the presence of background SRHA (Fig. 3b) due to the more negative zeta potential value. Unlike that present in NaCl solutions, the repulsive electrostatic interaction occurred between SRHA-adsorbed EPS and SRHA-adsorbed silica surface. The steric repulsion occurred between SRHA-adsorbed EPS and SRHA-adsorbed silica also contributed to the decreased EPS deposition kinetics in $CaCl_2$ solutions.

Similar to the observations in the presence of SRHA, α of both SEPS and BEPS for *E. coli* on bare silica surfaces in the presence of background alginate (1 mg L^{-1} TOC) (Fig. 4, grid bar) were also about 1–2 orders of magnitude lower than those in the absence of alginate (Fig. 4, black bar) in both NaCl and $CaCl_2$ solutions. Like SRHA, background alginate also adsorbed onto EPS surfaces in both NaCl and $CaCl_2$ solutions, which resulted in the more negative zeta potentials of EPS in the presence of background alginate (alginate-adsorbed EPS) relative to those in the absence of alginate (bare EPS) (Fig. 1). As a result, electrostatic interaction between EPS and silica is expected to be more repulsive with the presence of alginate relative to that without background alginate (Fig. 3c and

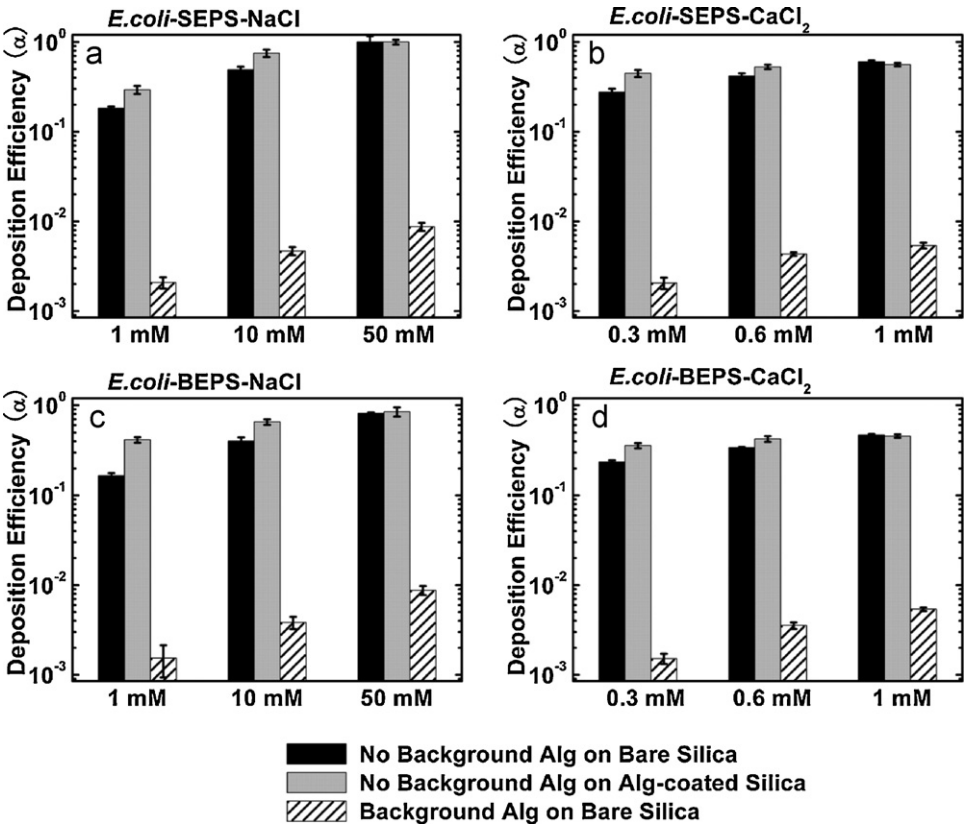

Fig. 4. Deposition efficiencies (α) of SEPS (a and b) and BEPS (c and d) extracted from *E. coli* in the absence of NOM on bare silica surfaces (black bar) and alginate-coated silica surfaces (gray bar), and in the presence of background alginate on bare silica surfaces (grid bar) as a function of ionic strength in NaCl (left) and $CaCl_2$ (right) solutions at pH 6.0 (adjusted with 0.1 M HCl or 0.1 M NaOH). Alg refers to alginate. Duplicate measurements were conducted over entire ionic strength range ($n \geq 2$), with error bars representing standard deviations.

d), causing the significant decrease of deposition kinetics in both NaCl and $CaCl_2$ solutions. Similar to that in the presence of SRHA, the electrostatic repulsive interaction occurred between alginate-adsorbed EPS and bare silica and between alginate-adsorbed EPS and alginate-adsorbed silica surface in NaCl and $CaCl_2$ solutions, respectively. Steric interaction occurring between EPS and silica surfaces would also contribute the reduced EPS deposition onto silica surfaces in the presence of alginate.

The decreased deposition kinetics with the presence of NOM (SRHA or alginate) in solutions was also observed for both SEPS and BEPS extracted from other three bacterial strains (Figs. S6 and S7). Above results indicate that, for all examined EPS regardless from which source they were extracted, the presence of dissolved NOM in solutions would significantly retard their deposition kinetics in both NaCl and $CaCl_2$ solutions.

4. Conclusion

This study showed that deposition of EPS, the ubiquitous biomacromolecules in natural environment, on silica surfaces could be significantly influenced by NOM under solution conditions relevant to subsurface environment. The deposition of EPS on silica surfaces could be retarded significantly (up to 1–2 orders of magnitude) even at humic acid and alginate concentration as low as 1 mg L^{-1} TOC via electrostatics and steric repulsion. However, pre-coated NOM on silica surfaces can either reduce or enhance the EPS deposition kinetics, depending on the surface morphology of the NOM macromolecules.

Acknowledgements

This work was supported by the National Natural Science Foundation of China-Young Scientists Fund under grant No. 40802054. This research was also in part supported by the National Research Foundation of Korea Grant funded by the Korean Government (MEST) (NRF-2010-0023782). The authors also wish to acknowledge Prof. Bengt Kasemo from Department of Physics at Chalmers University of Technology, Gothenburg for his useful comments. We acknowledge the editor and the reviewers for their very positive and helpful comments. We are also grateful to Professor Alistair Borthwick from the University of Oxford for his kind help in English editing.

Appendix A. Supplementary data

Supplementary data associated with this article can be found, in the online version, at doi:10.1016/j.colsurfb.2011.05.015.

References

[1] S.A. Welch, A.E. Taunton, J.F. Banfield, Geomicrobiol. J. 19 (2002) 343–367.
[2] B. Toner, A. Manceau, M.A. Marcus, D.B. Millet, G. Sposito, Environ. Sci. Technol. 39 (2005) 8288–8294.
[3] T.M. Lapara, J.E. Alleman, Water Res. 33 (1999) 895–908.
[4] T. Li, J. Liu, R. Bai, D.G. Ohandja, F.S. Wong, Water Res. 41 (2007) 3465–3473.
[5] C. Rodriguez-Navarro, C. Jimenez-Lopez, A. Rodriguez-Navarro, M.T. Gonzalez-Munoz, M. Rodriguez-Gallego, Geochim. Cosmochim. Acta 71 (2007) 1197–1213.
[6] R. Riding, Sedimentology 47 (2000) 179–214.
[7] M.J. Brown, J.N. Lester, Water Res. 16 (1982) 1539–1548.
[8] Y.M. Nelson, L.W. Lion, M.L. Shuler, W.C. Ghiorse, Environ. Sci. Technol. 30 (1996) 2027–2035.

[9] N. Yee, L.G. Benning, V.R. Phoenix, F.G. Ferris, Environ. Sci. Technol. 38 (2004) 775–782.
[10] J. Wingender, M. Strathmann, A. Rode, A. Leis, H.C. Flemming, Microbial Growth in Biofilms, PT A R Biological Aspects 336 (2001) 302–314.
[11] B. Frolund, R. Palmgren, K. Keiding, P.H. Nielsen, Water Res. 30 (1996) 1749–1758.
[12] G.P. Sheng, H.Q. Yu, Water Res. 40 (2006) 1233–1239.
[13] K.D. Kwon, V. Vadillo-Rodriguez, B.E. Logan, J.D. Kubicki, Geochim. Cosmochim. Acta 70 (2006) 3803–3819.
[14] S.N. Liss, I.G. Droppo, D.T. Flannigan, G.G. Leppard, Environ. Sci. Technol. 30 (1996) 680–686.
[15] S. Burdman, E. Jurkevitch, M.E. Soria-Diaz, A.M.G. Serrano, Y. Okon, FEMS Microbiol. Lett. 189 (2000) 259–264.
[16] J.A. Redman, S.L. Walker, M. Elimelech, Langmuir 38 (2004) 1777–1785.
[17] M. Tong, T.A.W.P. Camesano, Environ. Sci. Technol. 39 (2005) 3679–3687.
[18] L. Yang, C.H. Yang, J. Li, Environ. Sci. Technol. 41 (2007) 198–205.
[19] S. Tsuneda, H. Aikawa, H. Hayashi, A. Yuasa, A. Hirata, FEMS Microbiol. Lett. 223 (2003) 287–292.
[20] G. Long, P. Zhu, Y. Shen, M. Tong, Environ. Sci. Technol. 43 (2009) 2308–2314.
[21] A. Omoike, J. Chorover, K.D. Kwon, J.D. Kubicki, Langmuir 20 (2004) 11108–11114.
[22] K.D. Kwon, H. Green, P. Bjoorn, J.D. Kubicki, Environ. Sci. Technol. 40 (2006) 7739–7744.
[23] P. Zhu, G. Long, J. Ni, M. Tong, Environ. Sci. Technol. 43 (2009) 5699–5704.
[24] B. Yuan, M. Pham, T.H. Nguyen, Environ. Sci. Technol. 42 (2008) 7628–7633.
[25] M. Pham, E.A. Mintz, T.H. Nguyen, J. Colloid Interface Sci. 338 (2009) 1–9.
[26] K.L. Chen, M. Elimelech, Environ. Sci. Technol. 42 (2008) 7607–7614.
[27] N.A. Wall, G.R. Choppin, Appl. Geochem. 18 (2003) 1573–1582.
[28] J.B. Fein, J.F. Boily, K. Guclu, E. Kaulbach, Chem. Geol. 162 (1999) 33–45.
[29] A. Franchi, C.R. O'Melia, Environ. Sci. Technol. 37 (2003) 1122–1129.
[30] W.P. Johnson, G.L. Amy, Environ. Sci. Technol. 29 (1995) 807–817.
[31] L.M. Mosley, K.A. Hunter, W.A. Ducker, Environ. Sci. Technol. 37 (2003) 3303–3308.
[32] W.R. Gombotz, S.F. Wee, Adv. Drug Deliv. Rev. 31 (1998) 267–285.
[33] T.A. Davis, F. Llanes, B. Volesky, A. Mucci, Environ. Sci. Technol. 37 (2003) 261–267.
[34] J. Manka, M. Rebhun, Water Res. 16 (1982) 399–403.
[35] K.L. Chen, M. Elimelech, Langmuir 22 (2006) 10994–11001.
[36] T.H. Nguyen, M. Elimelech, Biomacromalecules 8 (2007) 24–32.
[37] J.V. Jester, M.M. Rodrigues, I.M. Herman, Am. J. Pathol. 127 (1987) 140–148.
[38] L.W. Mays, Water Resources Handbook, 1996.
[39] A.J. de Kerchove, M. Elimelech, Macromolecules 39 (2006) 6558–6564.
[40] A.J. de Kerchove, P. Weronski, M. Elimelech, Langmuir 23 (2007) 12301.
[41] R. Hogg, T.W. Healy, D.W. Ferstenau, Trans. Faraday Soc. 62 (1966) 1638–1651.
[42] J. Bergendahl, D. Grasso, AIChE J. 45 (1999) 475–484.
[43] J.N. Israelachvili, Intermolecular and Surface Forces, 2nd ed., Academic Press, London, 1992.
[44] J.J. Valle-Delgado, J.A. Molina-Bolivar, F. Galisteo-Gonzalez, M.J. Galvez-Ruiz, A. Feiler, M.W. Rutland, J. Phys. Chem. B 108 (2004) 5365–5371.
[45] J.D. Hu, Y. Zevi, X.-M. Kou, J. Xiao, X.-J. Wang, Y. Jin, Sci. Total Environ. 408 (2010) 3477–3489.
[46] W. Khemakhem, E. Ammar, A. Bakhrouf, World J. Microbiol. Biotechnol. 21 (2005) 1623–1631.
[47] M.E. Parent, D. Velegol, Colloids Surf. B: Biointerf. 39 (2004) 45–51.
[48] K.L. Chen, S.E. Mylon, M. Elimelech, Environ. Sci. Technol. 40 (2006) 1516–1523.
[49] S.K. Hong, M. Elimelech, J. Membr. Sci. 132 (1997) 159–181.
[50] L.C. Xu, V. Vadillo-Rodriguez, B.E. Logan, Langmuir 21 (2005) 7491–7500.
[51] A.J. de Kerchove, M. Elimelech, Langmuir 24 (2008) 3392–3399.
[52] A.J. de Kerchove, M. Elimelech, Appl. Environ. Microbiol. 73 (2007) 5227–5234.